JOURNAL OF MATERIALS SCIENCE 32 (1997) 6021–6027

The effect of ternary addition of silicon on the structure and microstructure of rapidly solidified equiatomic TiNi alloys

R. NAGARAJAN, S. MANJINI, K. CHATTOPADHYAY
Department of Metallurgy, Indian Institute of Science, Bangalore 560 012, India

K. AOKI
Department of Materials Science, Kitami Institute of Technology, Kitami, Hokkaido 090, Japan

The influence of a small amount of silicon (up to 6 at %) on the structure and microstructure of rapidly solidified equiatomic TiNi alloys is reported. It is shown that a small amount of silicon suppresses the B2 TiNi formation and promotes a competitive nucleation of Ti_2Ni phase. Further additions of silicon promote the formation of glass. The behaviour of the ternary replacement of both titanium and nickel by silicon has been studied. It is shown that replacement of titanium increases the tendency for the formation of silicide phases while the latter is absent when silicon replaces the nickel atoms.

1. Introduction

The intermetallic TiNi has an ordered B2 structure and can form directly from the liquid state. Although equiatomic in composition, it has a range of existence, with a maximum range of 49.5–57 at % Ni at 1391 K [1]. At lower temperature, TiNi undergoes martensitic transformation, leading to the development of shape-memory alloys. Thermodynamic calculations for glass formation [2, 3] indicate a wide composition range where the formation of metallic glass is feasible. These extend beyond the TiNi composition in both the titanium- and nickel-rich ends. Rapid solidification experiments, however, indicate that glass does not form at the equiatomic composition. Reports indicate that addition of silicon promotes easy glass formation in Ti–Ni alloy [4–6]. It is reported that addition of 10 at % Si to equiatomic alloy promotes the formation of glass [4]. Recent works on rapid solidification of the equiatomic alloy, on the other hand, have shown that a small addition of silicon can suppress the formation of TiNi [7]. This promotes the competitive nucleation of the intermetallic compound Ti_2Ni. In the light of the above results, a need is felt for a systematic study of the alloying behaviour of a small addition of silicon under rapid solidification conditions. In the present communication we report the result of such a study.

Silicon can replace both titanium and nickel with compositions moving towards the nickel and titanium-rich ends, respectively. For each case, we have studied three alloys with increasing silicon content and carried out detailed structural and microstructural investigations.

2. Experimental procedure

The alloys were prepared from high-purity constituent elements (>99.999% purity) by arc melting under vacuum. The compositions of the alloys are given in Table I. Additional studies were carried out with $Ti_{50}Ni_{50}$ alloys with 0.3 at % Si and without any silicon. The rapid solidification processing of the alloys was carried out by the melt-spinning technique under vacuum with the surface velocity of the wheel maintained at 40 $m\,s^{-1}$. The melt-spun ribbons were subsequently characterized by X-ray diffraction (XRD) and transmission electron microscopic techniques (TEM). A JEOL 2000FXII transmission electron microscope operating at 200 kV, was employed for electron microscopy. The specimens for electron microscopy were prepared by the ion-beam thinning technique using a Gatan Ion-Beam Thinning unit. The thermal stability of the samples was studied by differential scanning calorimetry using a Perkin–Elmer DSC IIC under flowing argon gas.

3. Results

Fig. 1 shows the X-ray diffractograms of the silicon-containing samples, where silicon replaced titanium. Besides a broad peak, the diffraction pattern of the sample containing 1 at % Si shows a crystalline peak of B2 TiNi and Ti_2Ni. Increasing the silicon to 2 and 4 at % Si gave patterns containing only a single broad peak. Fig. 2 shows XRD patterns for alloys where silicon has replaced nickel. The sample containing 2 at % Si in this case exhibits, in addition to a broad peak, peaks of B2 TiNi. For the samples containing

0022–2461

TABLE I Alloy composition and the phases present in the as-spun condition in the six Ti–Ni–Si alloys

Composition	X-ray results	TEM results
$Ti_{50}Ni_{48}Si_2$	B2 TiNi + broad peak	B2 TiNi + Ti_2Ni
$Ti_{50}Ni_{46}Si_4$	Amorphous-like broad peak	Amorphous phase + fine dispersions of unidentified phase
$Ti_{50}Ni_{44}Si_6$	Amorphous-like broad peak	Amorphous
$Ti_{49}Ni_{50}Si_1$	B2 TiNi + Ti_2Ni	B2 TiNi + Ti_2Ni
$Ti_{48}Ni_{50}Si_2$	Amorphous	Amorphous + Ti_2Ni
$Ti_{46}Ni_{50}Si_4$	Amorphous	Amorphous + Ti_5Si_3

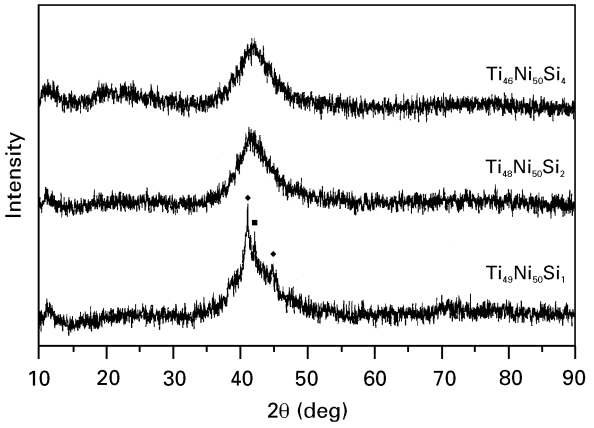

Figure 1 Powder X-ray diffraction patterns of melt-spun $Ti_{50-x}Ni_{50}Si_x$ alloys with $x = 1, 2$ and 4. (◆) Ti_2N, (■) TiNi.

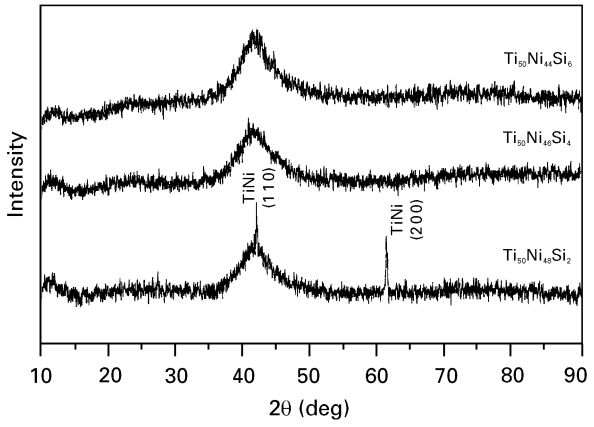

Figure 2 Powder X-ray diffraction patterns of melt-spun $Ti_{50}Ni_{50-x}Si_x$ alloys with $x = 2, 4$ and 6.

4 and 6 at % Si, the powder patterns exhibit a single broad and diffuse peak. In order to gain a clearer understanding of the phases present, TEM studies of the as-spun samples were carried out. Fig. 3 shows the TEM of an as-spun sample of $Ti_{50}Ni_{50}$ without any silicon. The micrograph shows a martensitic structure that is confirmed by the electron diffraction pattern. Even a small amount of silicon changes the microstructure drastically. Fig. 4 shows the micrograph of a sample containing 0.3 at % Si. The microstructure

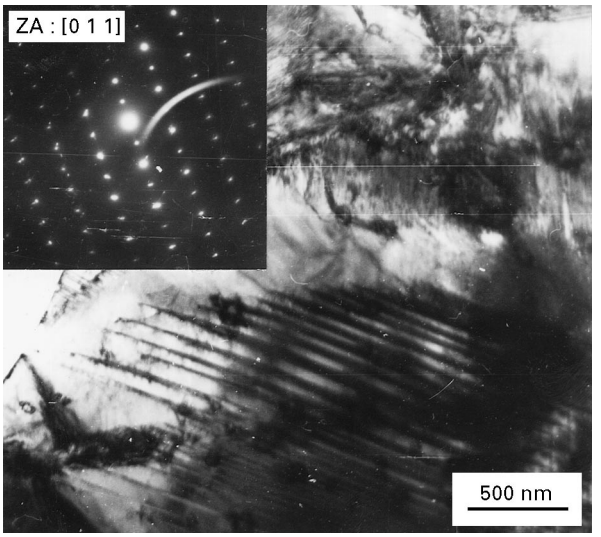

Figure 3 Bright-field micrograph of rapidly solidified $Ti_{50}Ni_{50}$ alloy indicating the presence of martensites of TiNi. The inset shows the [0 1 1] zone of the monoclinic martensitic phase.

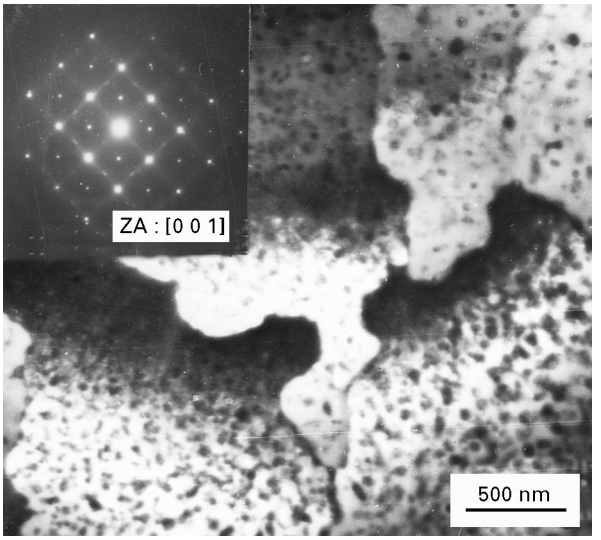

Figure 4 Bright-field micrograph of $Ti_{50}Ni_{50}$ rapidly solidified alloy containing 0.3 at % Si. The martensitic phase is completely absent. The fine dispersions are Ti_2Ni phase and the matrix is B2 ordered TiNi phase. The inset shows the [0 0 1] zone of B2 TiNi.

now consists of a matrix of B2 TiNi with Ti_2Ni particles dispersed within the matrix. Fig. 5 shows the morphology of the rapidly solidified alloy containing 2 at % Si replacing the nickel atoms. The microstructures still show a crystalline matrix. The selected-area diffraction patterns (SAD) show the single-crystal patterns of B2 TiNi matrix with superimposed broad crystalline rings that most probably belong to the Ti_2Ni phase. Increasing the silicon content to 4 at % Si results in an amorphous matrix with very fine unidentified particles embedded in it (Fig. 6a). The inset shows a typical electron diffraction pattern from the region, clearly showing the presence of the amorphous phase. The crystalline Debye rings are very broad. This prevents unique identification of the nature of the dispersoids. Increasing the silicon

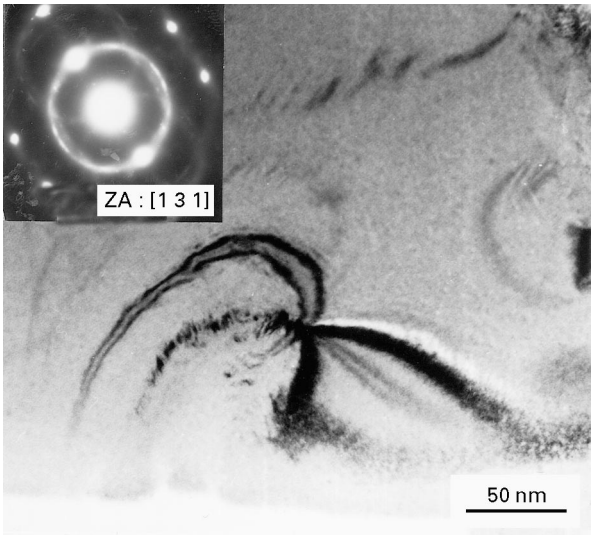

Figure 5 As-spun bright-field micrograph of $Ti_{50}Ni_{50}$ alloy with 2 at % Si replacing the nickel. The nanodispersion of Ti_2Ni phase in the TiNi matrix can be clearly seen. The inset shows the typical diffraction pattern. The spots belong to the [1 3 1] zone of TiNi. The rings belong to Ti_2Ni.

content further to 6 at % Si shows only amorphous phase (Fig. 6b).

The replacement of titanium by 1 at % Si shows a slightly different behaviour. The microstructure is characterized by the presence of nodular domains (Fig. 7a). The selected-area diffraction patterns from these domains reveal a single-crystal pattern of B2 TiNi with ring patterns of Ti_2Ni superimposed on it (Fig. 7b). Tilting the samples away from the B2 diffraction condition reveals clear rings of Ti_2Ni (Fig. 7c). Dark-field imaging using the B2 reflection illuminates the nodule (Fig. 7d), while dark-fields from the rings reveal the fine particles of Ti_2Ni (Fig. 7e). Increasing the silicon content to 2 at % results in a change in the diffraction pattern which now contains the Ti_2Ni Debye rings together with a strong diffuse ring due to amorphous phase (Fig. 8a). Fig. 8b shows a typical bright-field image. The dark-field imaging from the crystalline rings illuminate fine particles of Ti_2Ni embedded in the amorphous matrix (Fig. 8c). Increasing the silicon content to 4 at % does not alter the microstructure significantly. It still contains a glassy matrix with fine crystalline particles embedded in it (Fig. 9a). However, the diffraction pattern indicates the presence of a silicide phase, TiSi (Fig. 9b). Table I summarizes the results on melt-spun samples.

The samples containing glassy phases were heated in the differential scanning calorimeter to determine the stability of the glass. Clear decomposition peaks can be observed. The results are summarized in Table II. The peak temperature in all cases is 865 ± 3 K. Only the $Ti_{50}Ni_{44}Si_6$ sample showed an additional peak at a higher temperature. The low silicon-containing samples do not show any peaks. The X-ray diffraction patterns from the samples quenched after the decomposition peak are shown in Fig. 10a and b. Table III summarizes the results of the phases observed in each case. For silicon replacing nickel, we observe only B2 TiNi phase after the heat treatment.

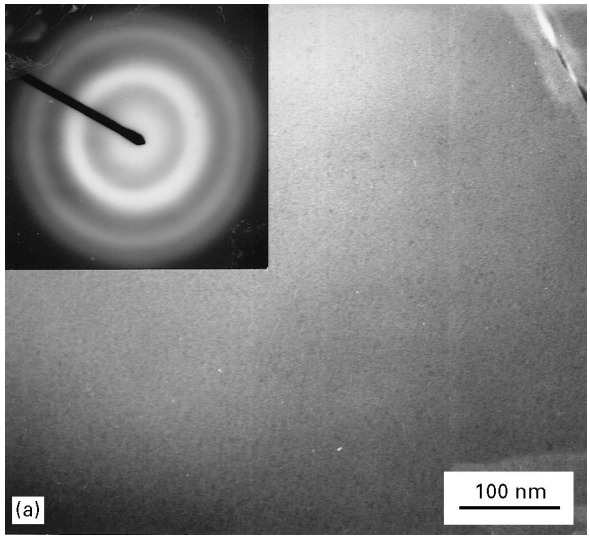

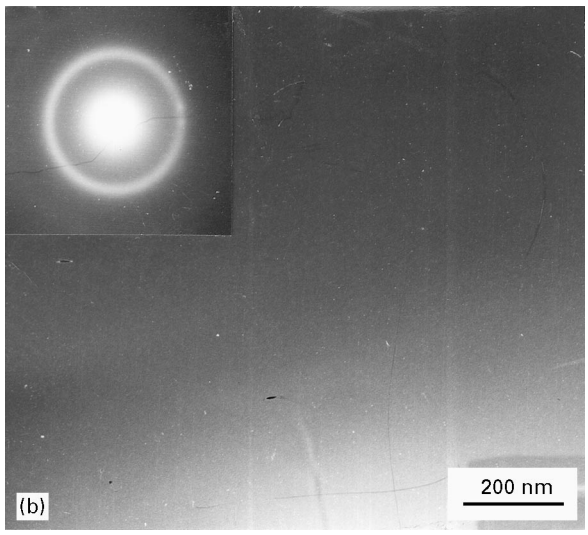

Figure 6 (a) Bright-field micrograph of the rapidly solidified $Ti_{50}Ni_{46}Si_4$ alloy showing fine particles dispersed in a featureless glassy matrix. The inset shows the diffraction pattern. The first broad ring is from the glassy phase. The other Debye rings are from crystalline dispersoids. (b) Bright-field micrograph of $Ti_{50}Ni_{44}Si_6$ alloy showing the contrastless feature of the glassy phase. The inset shows the electron diffraction pattern from the glassy phase.

However, in the samples where silicon replaces titanium, the peaks of Ti_2Ni together with two silicide phases TiSi and Ti_5Si_3, were observed in addition to the peaks of TiNi. We have carried out a Kissinger analysis to determine the activation energy for decomposition of the glassy phase in two samples ($Ti_{48}Ni_{50}Si_2$ and $Ti_{46}Ni_{50}Si_4$) by determining the shift of the peaks at different cooling rates. The Kissinger plots are shown in Fig. 11. The activation energy was found to be 78.4 and 79.4 kcal in the two cases, respectively.

4. Discussion

Small additions of silicon clearly have a major influence on the development of structure and microstructure in rapidly solidified Ti–Ni alloys. Silicon promotes the nucleation of Ti_2Ni intermetallic phase. The effect can be seen irrespective of whether silicon

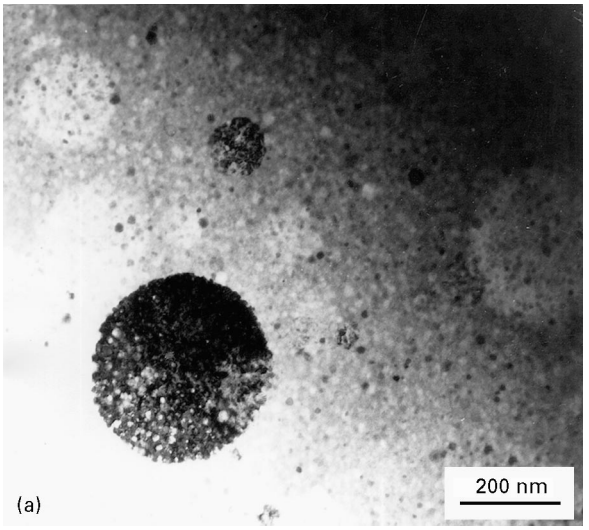

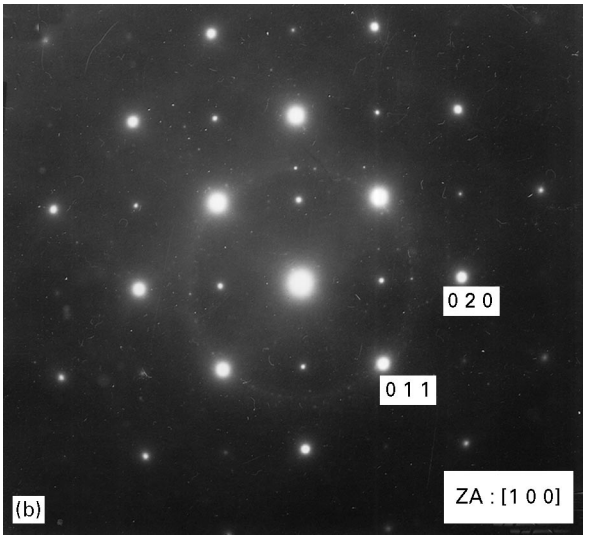

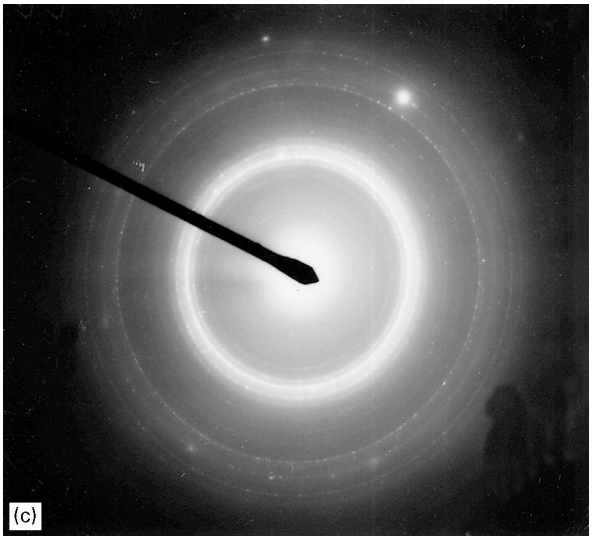

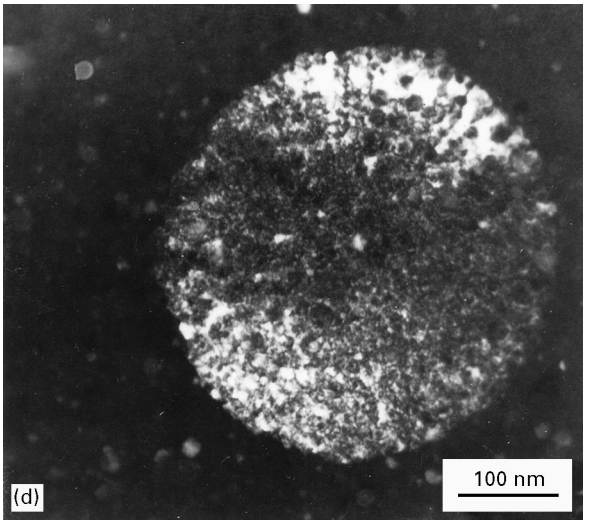

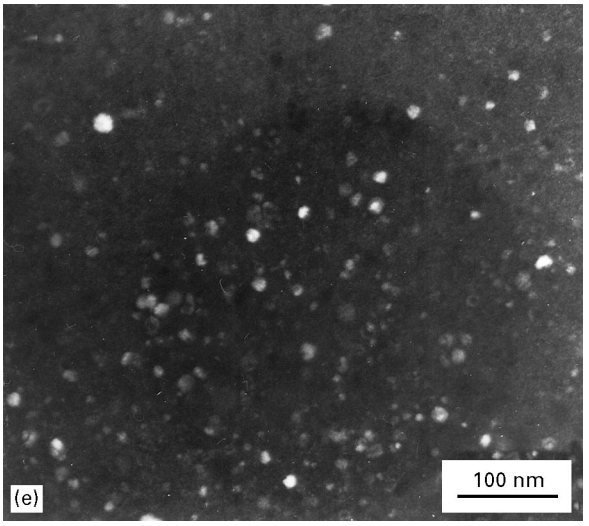

Figure 7 (a) A low-magnification micrograph of the as-spun $Ti_{50}Ni_{50}Si_1$ alloy showing the nodular morphology. (b, c) Selected-area electron diffraction pattern from the above, clearly showing the spot pattern of TiNi phase and the rings of Ti_2Ni phase respectively. All the rings can be uniquely identified as the Ti_2Ni phase. (d) Dark-field micrograph of the nodule using the [0 1 1] TiNi reflection. (e) The same region as above, imaged with a portion of the Ti_2Ni rings in (c).

replaces titanium or nickel. It is worthwhile to note that the as-solidified microstructure of the alloy where titanium is replaced by 1 at % Si, shows a spherical morphology of the B2 phase. These suggest an isotropic growth behaviour of the B2 phase and indicate free growth in the undercooled liquid. This emphasizes the role of silicon in promoting undercooling of the melt, even when it is present in a lower concentration. Such an undercooling enables the nucleation of Ti_2Ni to compete with the growth of TiNi phase. The appearance of glass with further silicon addition also indicates that it causes an increase in melt viscosity. This implies that the diffusion in the melt is retarded. This will reduce the growth rate of competing crystalline phases and will effectively reduce their sizes.

Our results suggest a difference in the alloying behaviour when silicon replaces titanium and nickel. In both cases small amounts promote a nanodispersion of Ti_2Ni phase in the B2 matrix. Further additions lead to the appearance of a glassy phase. The replacement of titanium by silicon is more effective in promoting glass. A 2 at % addition of silicon is sufficient for

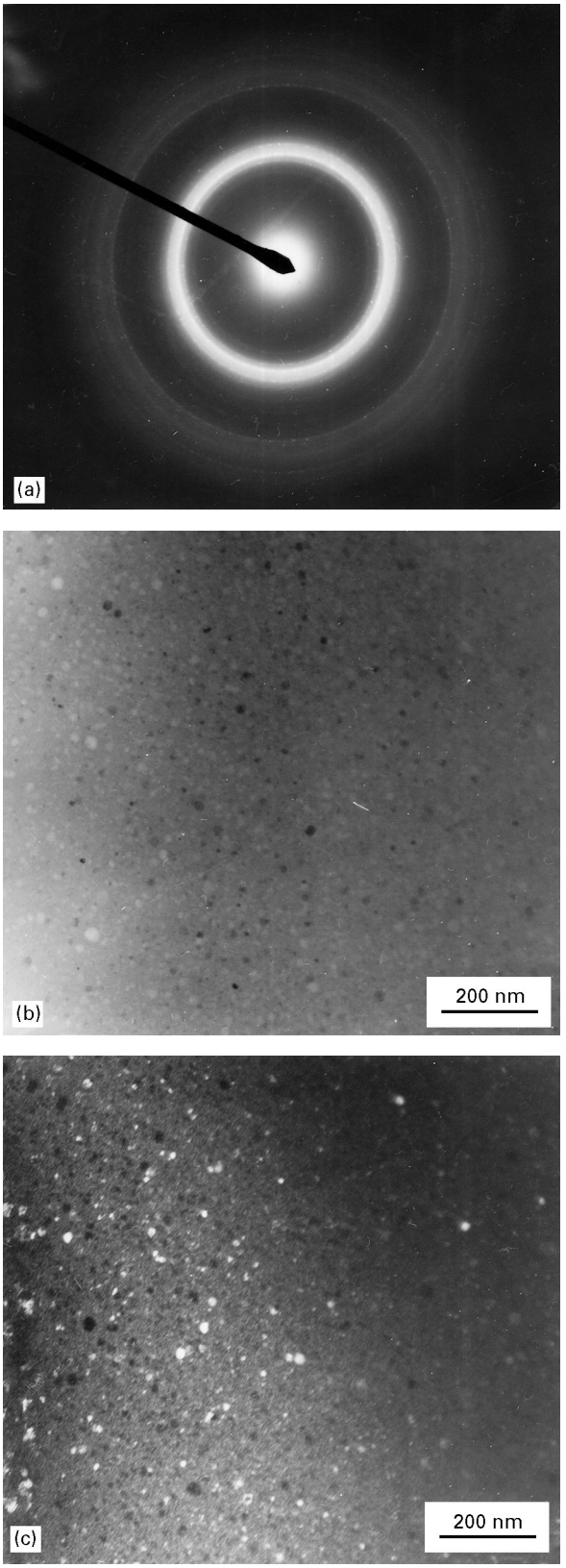

Figure 8 (a) A selected-area diffraction pattern of a rapidly solidified $Ti_{48}Ni_{50}Si_2$ alloy showing the presence of Ti_2Ni phase in a glassy matrix. (b) A bright-field micrograph of the region. Note the contrastless feature of the matrix, indicative of the glassy structure. (c) A dark-field micrograph using the Ti_2Ni rings illuminating the embedded fine particles.

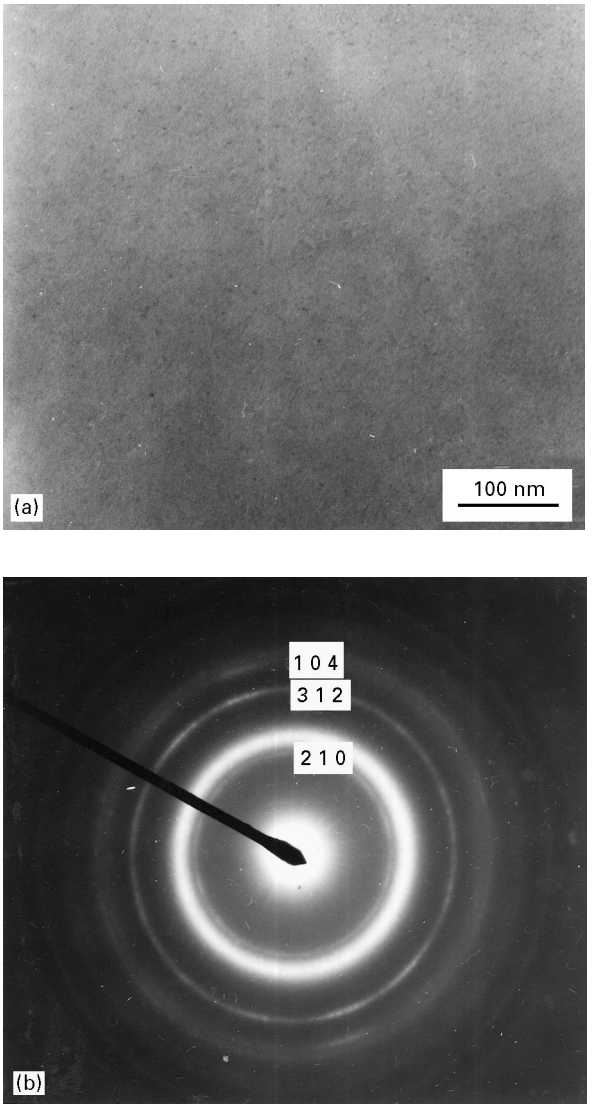

Figure 9 (a) Bright-field micrograph of rapidly solidified $Ti_{46}Ni_{50}Si_4$ alloy showing fine dispersed phase in a glassy matrix. (b) Selected-area diffraction pattern from the above, showing the presence of silicide phase (representative rings are indexed).

TABLE II Differential scanning calorimetric determination of the crystallization temperatures of the four alloys where glassy phase has been observed

Composition	T_{x1}(K)	T_{p1}(K)	T_{x2}(K)	T_{p2}(K)
$Ti_{50}Ni_{46}Si_4$	855	865	–	–
$Ti_{50}Ni_{44}Si_6$	854	862	902	919
$Ti_{48}Ni_{50}Si_2$	832	865	–	–
$Ti_{46}Ni_{50}Si_4$	858	867	–	–

[a] x, onset of peak.
[b] p, peak.

the glass to appear in the melt-spun foil when it replaces titanium. The same amount cannot promote glass when silicon replaces nickel. However, the TEM studies indicate that, in the case of titanium replacement, the glass coexists with second-phase dispersion. In $Ti_{48}Ni_{50}Si_2$ alloy it is Ti_2Ni, while in $Ti_{46}Ni_{50}Si_4$ alloy, a silicide phase, Ti_5Si_3 appears as a fine dispersion. Thus, glass formation competes with Ti_2Ni in the initial stage and with increasing silicon contents, the competing phase switches over to Ti_5Ni_3. The suppression of B2 phase is complete in both cases. The

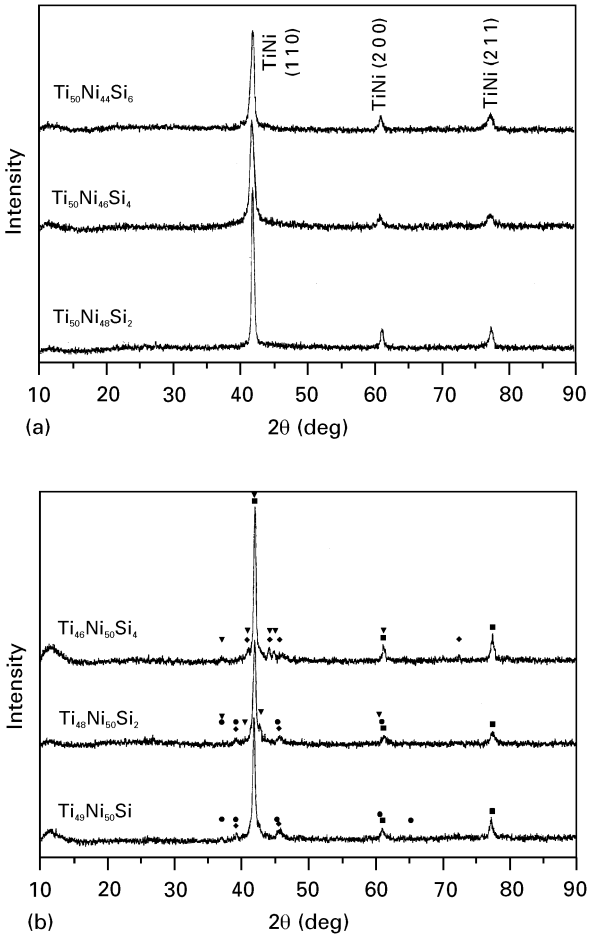

Figure 10 (a, b) X-ray diffractograms from the samples of the Ti–Ni–Si glassy alloys obtained by quenching in the DSC just after the decomposition peaks. (■) TiNi, (◆) Ti_2Ni, (●) TiSi, (▼) Ti_5Si_3.

TABLE III The X-ray diffraction identification of the phases present in the DSC quenched melt-spun samples of Ti–Ni–Si alloys after the appearance of the decomposition peaks

Composition	Phases observed
$Ti_{50}Ni_{48}Si_2$	B2 TiNi
$Ti_{50}Ni_{46}Si_4$	B2 TiNi
$Ti_{50}Ni_{44}Si_6$	B2 TiNi
$Ti_{49}Ni_{50}Si_1$	B2 TiNi + TiSi
$Ti_{48}Ni_{50}Si_2$	B2 TiNi + Ti_2Ni + Ti_5Si_3 + TiSi
$Ti_{46}Ni_{50}Si_4$	B2 TiNi + Ti_2Ni + Ti_5Si_3

replacement of nickel by silicon, on the other hand, promotes glass when the silicon content is 4 at % and above. The bright-field microstructures of the alloy having 4 at % Si addition still show a very fine dispersion which disappears when silicon is increased to 6 at %. The decomposition behaviour also shows a clear difference. In alloys where silicon replaces titanium, one always observes in the X-ray diffraction patterns silicide phases. These suggest that replacing titanium with silicon increases the tendency for the formation of silicide phase. For the case of silicon

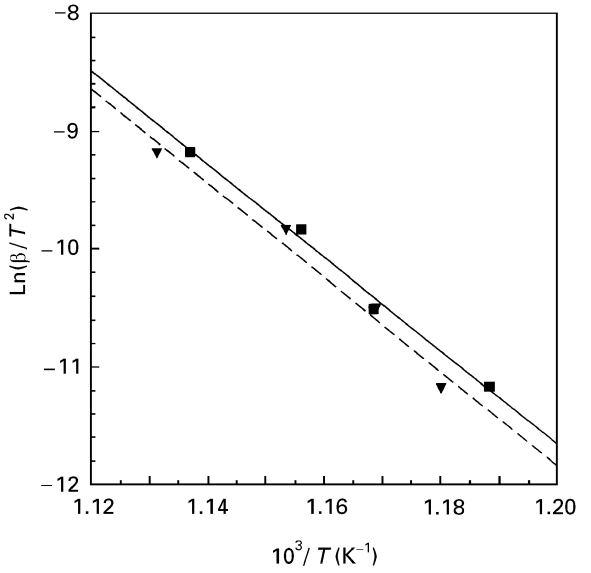

Figure 11 Kissinger plots to determine the activation energy for the decomposition of the glassy phase in the rapidly solidified (■) $Ti_{48}Ni_{50}Si_2$ (E_a = 78.4 kcal), (▼) $Ti_{46}Ni_{50}Si_4$ (E_a = 79.4 kcal).

replacing nickel, the X-ray diffraction of the decomposed product reveals only B2 TiNi peaks. In these cases, the silicon primarily influences the suppression of the B2 TiNi phase.

5. Conclusions

1. The addition of a small amount of silicon is effective in undercooling the melt and promotes competitive nucleation of TiNi phase under the condition of rapid solidification, yielding Ti_2Ni-dispersed TiNi nanocomposite. The range of silicon is 1 at % when it replaces the titanium atoms and 2 at % when it replaces nickel atoms.

2. Increasing the silicon content further suppresses the TiNi phase completely, and promotes the glass formation. For a small addition of silicon (up to 2 at % Si replacing nickel) the glass competes with Ti_2Ni and results in a fine dispersion of the latter.

3. The replacement of titanium by increasing amounts of silicon ($\geqslant$4 at %) leads to a glass with a fine dispersion of silicide phase.

4. The replacement of nickel by silicon promotes glass with no resolvable dispersion of second phase at a concentration of 6 at %. Below this concentration, the microstructure exhibits very fine dispersions that could not be identified.

5. The glassy phase decomposes with a single crystallization peak at 865 K. For nickel-rich alloys, the Kissinger analysis yields an activation energy of 79 kcal.

6. The X-ray characterization of the crystallization product for samples where silicon replaces nickel, reveals the presence of B2 TiNi intermetallic compounds.

7. In samples where silicon replaces titanium, in addition to TiNi phase, the presence of silicide phases is observed.

References

1. J. L. MURRAY, "The Ti–Ni Systems in Phase Diagram of Binary Titanium Alloys" (ASM International, Metals Park, OH, 1987) p. 197.
2. R. BORRMAN and K. ZOLZER, *Phys. Status Solidi*(*a*) **131** (1992) 691.
3. B. S. MURTY, S. RANGANATHAN and M. MOHAN RAO, *Mater. Sci. Eng.* **A149** (1992) 231.
4. D. E. POLK, A. CALKA and B. C. GIESSEN, *Acta Metall.* **26** (1978) 1097.
5. C. SURYANARAYANA, A. INOUE and T. MASUMOTO, in "Proceedings of the fourth International Conference on Titanium", edited by. H. Kumara and O. Izumi, Kyoto, Japan (1980) p. 699.
6. C. SEEGER and P. L. RYDER, *Mater. Sci. Eng.* **A179** (1994) 641.
7. R. NAGARAJAN and K. CHATTOPADHYAY, *Acta Metall. Mater.* **42** (1994) 947.

Received 19 April 1996
and accepted 17 April 1997